



Brazilian Journal of Physics

ISSN: 0103-9733

luizno.bjp@gmail.com

Sociedade Brasileira de Física
Brasil

Zhang, Zhi-Hong; Wu, Shao-Yi; Song, Bo-Tao; Zhang, Shan-Xiang
Theoretical Investigations on the Spin Hamiltonian Parameters and Local Structure for the Tetragonal
Pt³⁺ Center in BaTiO₃
Brazilian Journal of Physics, vol. 42, núm. 5-6, diciembre, 2012, pp. 340-346
Sociedade Brasileira de Física
São Paulo, Brasil

Available in: <http://www.redalyc.org/articulo.oa?id=46424644004>

- How to cite
- Complete issue
- More information about this article
- Journal's homepage in redalyc.org

redalyc.org

Scientific Information System
Network of Scientific Journals from Latin America, the Caribbean, Spain and Portugal
Non-profit academic project, developed under the open access initiative

Theoretical Investigations on the Spin Hamiltonian Parameters and Local Structure for the Tetragonal Pt^{3+} Center in $BaTiO_3$

Zhi-Hong Zhang · Shao-Yi Wu · Bo-Tao Song ·
Shan-Xiang Zhang

Received: 6 April 2012 / Published online: 6 July 2012
© Sociedade Brasileira de Física 2012

Abstract The spin Hamiltonian parameters (g factors and the hyperfine structure constants) and the local structure for the tetragonal Pt^{3+} center in $BaTiO_3$ are theoretically investigated from the improved perturbation formulas of these parameters for a $5d^7$ ion in a tetragonally elongated octahedron. The Jahn-Teller effect yields 0.05 Å longer $Pt^{3+} - O^{2-}$ bonds along the C_4 axis. Under the uniaxial [001] stress of 0.17 GPa, the impurity center shows a moderate decrease of 12% for the tetragonal elongation and a slight increase of 3% for the core polarization constant, leading to the decline of the anisotropy Δg ($= g_{\perp} - g_{\parallel}$) and the increase of ΔA ($= A_{\perp} - A_{\parallel}$), respectively. The calculated spin Hamiltonian parameters show good agreement with the observed values.

Keywords Impurity and defects ·
Electron paramagnetic resonance ·
 Pt^{3+} $BaTiO_3$

1 Introduction

$BaTiO_3$ is a ferroelectric with a number of interesting and important properties, such as dielectric [1], pyroelectric [2], ferroelectric [3–6], electric [7, 8], mechanic [9], optical [10, 11], photorefractive [12, 13], ferromagnetism [14] and structural properties [15, 16] which have been extensively investigated. On the other hand, transition-metal impurities (e.g., Pt^{3+}) can locally change the above properties by inducing unique impurity energy levels and related local distortions. In particular, it is well documented that Pt^{3+} usually suffers the Jahn-Teller effect in crystals [17–19], which correlates to removal of the degeneracy of energy levels via vibration interactions and results in lower symmetry and energy [20–22]. Electron paramagnetic resonance (EPR) is a powerful tool to study local distortions and electronic states of paramagnetic impurities in various hosts, and thus EPR investigations for Pt^{3+} in crystals (e.g., $BaTiO_3$) are of specific importance. EPR measurements were performed for $Pt^{3+}(5d^7)$ in rhombohedral $BaTiO_3$ at 4.2 K [17, 23, 24]. A phenomenological spin Hamiltonian was proposed to fit the observed EPR spectra, whose central line, under certain circumstances, was surprisingly less intense than the hyperfine satellites [17, 23, 24]. The corresponding spin Hamiltonian parameters (g factors g_{\parallel} and g_{\perp} and the hyperfine structure constants A_{\parallel} and A_{\perp}) were obtained for the tetragonal $^{195}Pt^{3+}$ center, and the tetragonality was attributed to the Jahn-Teller effect of this impurity center [17, 23, 24]. Up to now, however, theoretical and systematic computations (or quantitative explanations) of the above EPR experimental results have not been made, and no information about the local structure of this center has been determined yet.

Z.-H. Zhang · S.-Y. Wu (✉) · B.-T. Song · S.-X. Zhang
Department of Applied Physics, University of Electronic
Science and Technology of China, Chengdu 610054,
People's Republic of China
e-mail: shaoyi_wu@163.com

Z.-H. Zhang
e-mail: zhihongzhang723@163.com

S.-Y. Wu
International Centre for Materials Physics,
Chinese Academy of Sciences, Shenyang 110016,
People's Republic of China

In general, such information about EPR spectra and local structures of transition-metal ions in $BaTiO_3$ can be useful to understand the properties of this material with dopants. Pt^{3+} belongs to the strong crystal-field case of low spin ($S=1/2$), which is quite different from the weak crystal-field case of high spin ($S=3/2$) for conventional $3d^7$ (e.g., Co^{2+}) ions in oxides [25]. And studies of $Pt^{3+}(5d^7)$ in $BaTiO_3$ (or other ABO_3 perovskites) may provide different microscopic mechanisms of the EPR spectra from those of the conventional $3d^n$ ions and enhance the knowledge of EPR fields. Therefore, further theoretical investigations on the spin Hamiltonian parameters and the local structure for the Pt^{3+} center in $BaTiO_3$ are of scientific and practical significance. In this work, the improved perturbation formulas of the spin Hamiltonian parameters for a $5d^7$ ion in a tetragonally elongated octahedron are established, and a more basic calculation is presented for $BaTiO_3 : Pt^{3+}$, which interprets the spin Hamiltonian parameters. Comparison with experiment yields good agreement with a single adjustable parameter (i.e., the relative tetragonal elongation due to the Jahn-Teller effect).

2 Theory and Calculations

In the rhombohedral phase of $BaTiO_3$ at low temperature, host Ti^{4+} ion occupies an off-center site away from the center of oxygen octahedron [26]. When a Pt^{3+} ion enters the lattice of $BaTiO_3$, it may locate substitutionally on the octahedral Ti^{4+} site due to their similar size or charge. Although the host Ti^{4+} in rhombohedral $BaTiO_3$ has slight trigonal distortion arising from the eccentric site along [111] axis [26], the Jahn-Teller ion Pt^{3+} may experience the Jahn-Teller effect via stretching two $Pt^{3+} - O^{2-}$ bonds along [001] (or $C_4//Z$) axis and consequently transform the local symmetry from tiny trigonal to tetragonal (see Fig. 1). As a result, the $[PtO_6]^{9-}$ cluster actually exhibits a tetragonally elongated octahedron, and the original slight trigonal distortion can be completely concealed. The above tetragonal elongation is also found for the isoelectronic $Rh^{2+}(4d^7)$ in the same rhombohedral $BaTiO_3$ [17, 24] and Co^{4+} (with the same low spin $S=1/2$) in similar $SrTiO_3$ [22]. In addition, for Cu^{2+} on original trigonal Cd^{2+} site in $CsCdCl_3$, the $[CuCl_6]^{4-}$ cluster exhibits a similar tetragonally elongated octahedron of the Jahn-Teller nature [27]. Thus, the local structure of this center may be conveniently described by the relative tetragonal elongation ΔZ . In the following, improved perturbation formulas of the spin Hamiltonian parameters are established, with the related model parameters

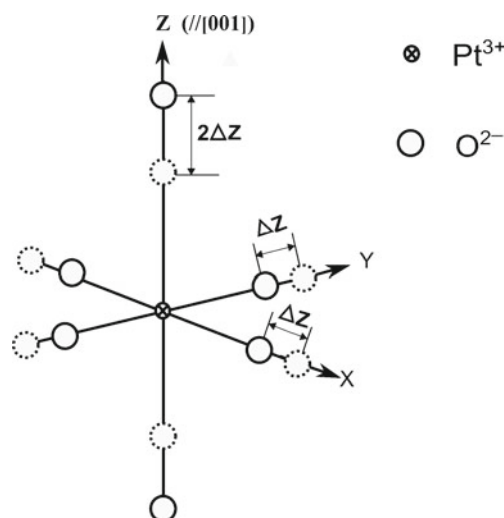


Fig. 1 Local structure of the tetragonal Pt^{3+} center in $BaTiO_3$. The dashed circles indicate the positions of the ligands in the undistorted cluster, while the solid-line circles show the Jahn-Teller distorted positions of the ligands. The impurity Pt^{3+} occupies the Ti^{4+} site, and the Jahn-Teller effect yields 0.05 Å longer $Pt^{3+} - O^{2-}$ bonds along the Z axis

theoretically determined from the cluster approach. A quantitative is then carried out for the EPR spectra and the local structure of $BaTiO_3 : Pt^{3+}$.

2.1 Perturbation Hamiltonian

When the ligand octahedron around the impurity $Pt^{3+}(5d^7)$ ion is elongated, the ground 2E_g state of cubic case would be separated into two orbital singlets ε (${}^2B_{1g}$) and θ (${}^2A_{1g}$), with the latter lying lowest (see Fig. 2) [15]. In order to establish improved expressions

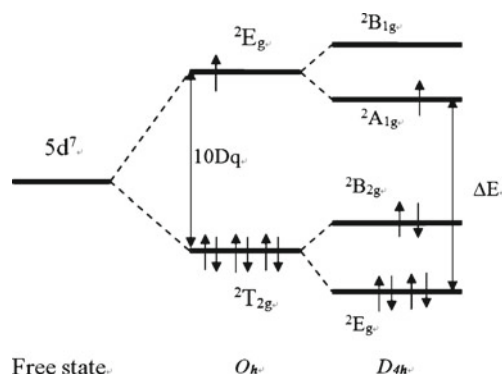


Fig. 2 The crystal-field level diagram for a $5d^7$ ion under tetragonally elongated octahedra. The central (O_h) and right-hand (D_{4h}) structures of the energy levels are associated with the undistorted and distorted cells, respectively

for the spin Hamiltonian parameters, the perturbation Hamiltonian may be taken as follows:

$$H' = H_{so}(\zeta, \zeta') + H_{Zeeman}(k, k') + H_{hyperfine}(P) + V_{tetra}(D_s, D_t), \quad (1)$$

where H_{so} , H_{Zeeman} , $H_{hyperfine}$ and V_{tetra} are, respectively, the spin-orbit coupling, the Zeeman term, the hyperfine interactions and the tetragonal crystal-field interactions, with the corresponding spin-orbit coupling coefficients ζ , ζ' , the orbital reduction factors k and k' , the dipolar hyperfine structure parameter P and the tetragonal field parameters D_s and D_t .

2.2 Spin-Orbit Coupling Coefficients and Orbital Reduction Factors of the Cluster Approach

In the previous treatments of spin Hamiltonian parameters for tetragonal $5d^7$ clusters [25, 28], the contributions of the ligand orbitals and spin-orbit coupling coefficient were not taken into account. As opposed to $3d^n$ ions, where covalency and ligand contributions have little influence on the g factors and the hyperfine structure constants, for Pt^{3+} they can no longer be ignored even in oxides. So, the above ligand contributions should be considered here in order to derive improved perturbation formulas. Based on the cluster approach, the single-electron wave functions including the contributions from both the central ion d-orbitals and the ligand s- and p-orbitals can be expressed in terms of linear combinations of atomic orbitals—molecular orbitals (LCAO-MO) [29]:

$$\begin{aligned} \psi_t &= N_t^{1/2}(\varphi_t - \lambda_t \chi_{pt}), \\ \psi_e &= N_e^{1/2}(\varphi_e - \lambda_e \chi_{pe} - \lambda_s \chi_s), \end{aligned} \quad (2)$$

where φ_γ ($\gamma = e$ and t denote the irreducible representations E_g and T_{2g} of the O_h group) are the d orbitals of the central ion. $\chi_{p\gamma}$ and χ_s stand for the p- and s-orbitals of the ligands. N_γ and λ_γ (or λ_s) are, respectively, the normalization factors and the orbital admixture coefficients.

In (1), the spin-orbit coupling coefficients ζ (and ζ') and the orbital reduction factors k (and k') denote the diagonal (and off-diagonal) matrix elements of the spin-orbit coupling and orbital angular momentum operators within the irreducible representations γ . They are usually determined from the cluster approach [29]:

$$\begin{aligned} \zeta &= N_t (\zeta_d^0 + \lambda_t^2 \zeta_p^0 / 2), \quad \zeta' = (N_t N_e)^{1/2} (\zeta_d^0 - \lambda_t \lambda_e \zeta_p^0 / 2), \\ k &= N_t (1 + \lambda_t^2 / 2), \quad k' = (N_t N_e)^{1/2} (1 - \lambda_t (\lambda_e + \lambda_s A) / 2), \end{aligned} \quad (3)$$

where ζ_d^0 and ζ_p^0 are the spin-orbit coupling coefficients of a free $5d^7$ and ligand ions, respectively. N_γ and λ_γ (or λ_s) are, respectively, the normalization factors and the orbital admixture coefficients. A is the integral $R \langle ns | \frac{\partial}{\partial y} | np_y \rangle$, where R stands for the impurity-ligand (reference) distance of the studied system. Utilizing the cluster approach [29], the molecular orbital coefficients N_γ and λ_γ (or λ_s) can be determined from the normalization conditions

$$\begin{aligned} N_t (1 - 2\lambda_t S_{dpt} + \lambda_t^2) &= 1, \\ N_e (1 - 2\lambda_e S_{dpe} - 2\lambda_s S_{ds} + \lambda_e^2 + \lambda_s^2) &= 1, \end{aligned} \quad (4)$$

and the approximate relationships

$$\begin{aligned} N^2 &= N_t^2 [1 + \lambda_t^2 S_{dpt}^2 - 2\lambda_t S_{dpt}], \\ N^2 &= N_e^2 [1 + \lambda_e^2 S_{dpe}^2 + \lambda_s^2 S_{ds}^2 - 2\lambda_e S_{dpe} - 2\lambda_s S_{dps}]. \end{aligned} \quad (5)$$

Here S_{dpy} (and S_{ds}) are the group overlap integrals. In general, the orbital admixture coefficients increase with increasing the group overlap integrals. Thus, one can approximately adopt the proportional relationship $\lambda_e / S_{dpe} \approx \lambda / S_{ds}$ between the orbital admixture coefficients and the related group overlap integrals within the same irreducible representation E_g .

2.3 Improved Formulas of the Spin Hamiltonian Parameters

The perturbation formulas of the spin Hamiltonian parameters of the lowest $^2A_{1g}$ state for a $5d^7$ ion in tetragonally elongated octahedra were established including the contributions from the metal spin-orbit coupling coefficient and orbital reduction factor [25, 28].

By applying the perturbation Hamiltonian in (1) to the basic functions in (2) by means of the perturbation method similar to that in Ref. [28], the improved formulas of the spin Hamiltonian parameters for a tetragonally elongated $5d^7$ cluster can be obtained as follows:

$$\begin{aligned} g_{\parallel} &= g_s \cos 2\alpha + 2k^2 \sin^2 \alpha, \\ g_{\perp} &= g_s \cos^2 \alpha + \sqrt{6} k^2 \sin 2\alpha, \\ A_{\parallel} &= P \left[-\kappa + 4N^2 / 7 - \sqrt{6} \sin 2\alpha / 7 + 8 \sin^2 \alpha / 7 \right], \\ A_{\perp} &= P \left[-\kappa - 2N^2 / 7 + 15\sqrt{6} \sin 2\alpha / 14 - 4 \sin^2 \alpha / 7 \right], \end{aligned} \quad (6)$$

with

$$\alpha = tg^{-1} \left[\sqrt{6} \zeta' / (\zeta / 2 - \Delta E) \right] / 2. \quad (7)$$

Here g_s ($=2.0023$) is the spin-only value. P and A are the dipolar hyperfine structure parameter and the core polarization constant, respectively. $\Delta E (= 10D_q - D_s - 10D_t)$ is the energy separation between the ground $^2A_{1g}$ and the excited 2E_g states. Here D_q is the cubic field parameter, and D_s and D_t are the tetragonal ones. N is the average covalency factor, characteristic of the covalency (orbital admixtures) between the impurity and ligand ions.

2.4 Crystal-field parameters

Unlike the previous treatments [25, 28], where the low symmetrical (tetragonal) distortion was ignored, the local elongation due to the Jahn-Teller effect is quantitatively taken into account for the tetragonal $[PtO_6]^{9-}$ cluster here. The parallel and perpendicular bond lengths can be expressed in terms of the reference distance R and the relative elongation ΔZ as $R_{\parallel} \approx R + 2\Delta Z$ and $R_{\perp} \approx R - \Delta Z$ (see Fig. 1). The tetragonal field parameters are determined from the superposition model [30]:

$$D_s \approx (4/7)\bar{A}_2(R) [(R/R_{\perp})^{t_2} - (R/R_{\parallel})^{t_2}],$$

$$D_t \approx (16/21)\bar{A}_4(R) [(R/R_{\perp})^{t_4} - (R/R_{\parallel})^{t_4}]. \quad (8)$$

Here t_2 (≈ 3) and t_4 (≈ 5) are the power-law exponents [30]. $\bar{A}_2(R)$ and $\bar{A}_4(R)$ are the intrinsic parameters. For transition-metal ions in octahedra, the relationships $\bar{A}_4(R) \approx (3/4)D_q$ and $\bar{A}_2(R) \approx 10.8 \bar{A}_4(R)$ have been proved valid in many crystals [31–34]. Therefore, the spin Hamiltonian parameters (particularly the anisotropy $\Delta g (= g_{\perp} - g_{\parallel})$) are correlated to the tetragonal field parameters and hence to the local structure of the impurity center.

2.5 Calculations

Normally, the reference distance R can be different from the corresponding cation-anion distance ($\approx 2.002 \text{ \AA}$ [26]) in pure $BaTiO_3$ due to the size and charge

mismatching substitution of the host Ti^{4+} by the impurity Pt^{3+} . According to the studies based on experimental superhyperfine constant and extended X-ray absorption fine structure (EXAFS) measurements, the empirical formula $R \approx R_H + (r_i - r_h)/2$ is approximately valid for an impurity ion in crystals [35]. Here r_i ($\approx 0.72 \text{ \AA}$ [36]) is the ionic radii of the impurity Pt^{3+} and r_h ($\approx 0.68 \text{ \AA}$ [37]) is that of the host Ti^{4+} . Thus the distance R for the tetragonal Pt^{3+} center in rhombohedral $BaTiO_3$ is obtained and shown in Table 1. From the reference distance R and the Slater-type self-consistent field (SCF) functions [37, 38], the group overlap integrals are calculated and listed in Table 1. Since the spectral parameters for $BaTiO_3 : Pt^{3+}$ are not reported, the values of D_q and N [39] for the similar $[PtO_6]^{9-}$ cluster in $\alpha - Al_2O_3$ have been adopted. The molecular orbital coefficients are determined from (4) and (5) and collected in Table 1. Using the free-ion values $\zeta_d^0 \approx 5011 \text{ cm}^{-1}$ [40] for Pt^{3+} and $\zeta_p^0 \approx 151 \text{ cm}^{-1}$ [41] for O^{2-} , the spin-orbit coupling coefficients and the orbital reduction factors are acquired from (3) and listed in Table 1. The dipolar hyperfine structure parameter is $P \approx 425 \times 10^{-4} \text{ cm}^{-1}$ [42] for $^{195}Pt^{3+}$. In the formulas of the hyperfine structure constants, the core polarization constant can be determined from the relationship $\kappa \approx -2N\chi/(3\langle r^{-3} \rangle)$ [28], where χ is characteristic of the unpaired spin density at the nucleus of the central ion and $\langle r^{-3} \rangle$ is the expectation value of the inverse cube of the 5d radial wave function. Applying the data $\langle r^{-3} \rangle \approx 13.74 \text{ a.u.}$ [43] for Pt^{3+} and $\chi \approx -10 \text{ a.u.}$ [28] for $5d^7$ ions in crystals, the value of κ is determined for $BaTiO_3 : Pt^{3+}$ here and also shown in Table 1. This value is close to the result ($0.26 - 0.3$ [44]) for some $3d^7$ ions (e.g., Co^{2+}) in tutton salts and that (≈ 0.26 [45]) for Co^{2+} in halides and can be regarded as suitable.

There is only one unknown parameter, the relative tetragonal elongation ΔZ , in the formulas of the spin Hamiltonian parameters. Substituting the above values into (6) and fitting the calculated results to the exper-

Table 1 The reference distances R (in \AA), the cubic field parameter D_q (in cm^{-1}), the average covalency factor N , the group overlap integrals S_{dpt} , S_{dpe} , S_{ds} and A , the molecular orbital coefficients N_t , N_e , λ_t , λ_e and λ_s , the spin-orbit coupling

X	R	S_{dpt}	S_{dpe}	S_{ds}	A	D_q	N	N_t	N_e
$BaTiO_3 : Pt^{3+}$	2.022	0.0156	0.0487	0.0390	1.3034	2500	0.6	0.608	0.633
X	λ_t	λ_e	λ_s	ζ	ζ'	k	k'	κ	ΔZ
$BaTiO_3 : Pt^{3+}$	0.819	0.646	0.517	3169	3008	0.812	0.285	0.29	0.05

coefficients ζ and ζ' (in cm^{-1}), the orbital reduction factors k and k' , and the core polarization constant as well as relative tetragonal elongation ΔZ (in \AA) for $BaTiO_3 : Pt^{3+}$

imental data, one can obtain the optimal value of ΔZ which is shown in Table 1. The corresponding results (labeled Calc. [(6)]) based on the improved formulas are given in Table 1. For comparison, the theoretical spin Hamiltonian parameters (Calc. (conventional)) based on the conventional formulas including only the metal orbital and spin-orbit coupling contributions (i.e., $k = k' = N$ and $\zeta = \zeta' = N\zeta_d^0$, similar to the previous treatments [25, 28]) are also shown in Table 1.

3 Discussion

Table 1 shows that the theoretical spin Hamiltonian parameters (Calc. [(6)]) based on the improved formulas (6) and the Jahn-Teller elongation ΔZ are in good agreement with the experimental data for the tetragonal Pt^{3+} center in $BaTiO_3$. Thus, the EPR spectra of the above impurity center are satisfactorily interpreted, and information of the local structure is also obtained (Table 2).

3.1 Local structure of the Pt^{3+} centers

The positive sign of the tetragonal elongation ΔZ is consistent with the expectation based on the Jahn-Teller elongation distortion for an octahedral $5d^7$ cluster. Meanwhile, the small ΔZ ($\approx 0.05\text{\AA}$) is also in accordance with the slight anisotropy (≈ 0.5 [17, 23, 24]). According to (6)–(8), ΔZ may bring forward the influences on the tetragonal distortion (D_s and D_t) and the energy denominator E and hence on the resultant spin Hamiltonian parameters. Similar tetragonal elongations of the ligand octahedra surrounding a d^7 impurity were also reported for Pt^{3+} in MgO [18] and Rh^{2+} in $AgCl$ [46] and $NaCl$ [47] due to the Jahn-Teller effect. Further, the above local elongation can entirely depress the slight trigonal distortion of the original Ti^{4+} site in rhombohedral $BaTiO_3$, as mentioned for the similar tetragonal Cu^{2+} center (arising from the Jahn-Teller effect) on the original trigonal Cd^{2+} site in $CsCdCl_3$ [27]. It seems that Pt^{3+} ions under octahedral

environments tend to suffer tetragonal elongation distortions and thus exhibit lower g_{\parallel} (< 2).

3.2 Covalency of the System

The studied Pt^{3+} center exhibits significant covalency and impurity-ligand orbital admixtures even in oxides, which can be illustrated by the low covalency factor N ($\approx 0.6 \ll 1$) and the obvious orbital admixture coefficients ($\approx 0.4 \sim 0.6$). When the ligand orbital and spin-orbit coupling contributions are neglected, the theoretical g factors (particularly g) are smaller than the observed values and thus yield lower g and the average $\bar{g} = (2g_{\perp} + g_{\parallel})/3$. Moreover, the above discrepancies can hardly be removed by modifying ΔZ , since variations of the tetragonal elongation affect mainly the local distortion (D_s and D_t) and cannot compensate the decrease of \bar{g} under omission of the ligand contributions. In fact, the relative deviations of about 103% and 4% are obtained for the orbital reduction factors and the spin-orbit coupling coefficients from the present cluster approach calculations. Therefore, the ligand contributions should be taken into account in the analysis of the spin Hamiltonian parameters for Pt^{3+} in $BaTiO_3$ (or similar ABO_3 perovskites).

3.3 Hyperfine Structure Constants

The core polarization constant κ usually accounts for the isotropic contributions to the hyperfine interactions from the Fermi contact term between the ground $5s^25d^7$ configuration and the excited s-orbitals (e.g., $5s5d76s$ states) of the central ion in crystals [25]. The adopted κ (≈ 0.29) for the studied system is consistent with the moderate Pt^{3+} 5d-5s (or 5d-6s) orbital admixtures and can be regarded as suitable. In addition, the A factors are found to be insensitive to the covalency or ligand contributions as compared with the g factors. From (6), the dominant contributions to the hyperfine structure constants arise from the isotropic part (related to κ), while the minor anisotropic parts (related to the angle α) depend upon the local structure (tetragonal

Table 2 The anisotropic g factors and the hyperfine structure constants (in 10^{-4} cm^{-1}) for the tetragonal Pt^{3+} center in $BaTiO_3$ at 4.2 K

	Zero stress				Uniaxial [001] stress of 0.17 GPa			
	g_{\parallel}	g_{\perp}	A_{\parallel}	A_{\perp}	g_{\parallel}	g_{\perp}	A_{\parallel}	A_{\perp}
Calc. [(6)]	1.939	2.268	−5.0	110.0	1.940	2.268	−4.8	113.8
Calc.(conventional)	1.950	2.450	−5.2	110.7	1.950	2.450	−4.8	114.5
Expt. [17, 23, 24]	1.958(5)	2.455(5)	~ 0	111.0(5)	1.958(5)	2.452(5)	~ 0	115.0(5)

distortion) of the system. Therefore, the influence of the ligand contributions is insignificant for the hyperfine structure constants.

3.4 Stress Dependences of the Spin Hamiltonian Parameters

Under the uniaxial [001] stress of 0.17 GPa [17], the EPR spectra of the Pt^{3+} center in $BaTiO_3$ yield slightly lower g_{\perp} (≈ 2.452) and higher A_{\perp} (≈ 115.0 ($5 \times 10^{-4} \text{ cm}^{-1}$)) and hence smaller anisotropy g and larger $\Delta A (= A_{\perp} - A_{\parallel})$. Fitting the above experimental results, one can obtain the optimal tetragonal elongation $\Delta Z \approx 0.044 \text{ \AA}$ and the core polarization constant 0.3, indicating a moderate decrease of 12% for ΔZ and a slight increase of 3% for κ . The decline of g reflects the reduction of the local tetragonal distortion due to the uniaxial [001] stress which may somewhat depress the original Jahn-Teller elongation. Nevertheless, the increase of ΔA can be attributed to the slightly more significant Pt^{3+} 5d-5s (or 5d-6s) orbital admixtures for the ground state $\theta(d_{z^2})$ under the uniaxial stress, which leads to the tiny increase of κ .

3.5 Error Analysis

Consider now the error in our calculation. First, the approximation of the theoretical model and the perturbation formulas adopted in this work can introduce deviations. The calculations are carried out from the cluster approach containing only the six nearest neighbouring oxygen ligands, while the influence of the rest of the lattice is ignored. This approximation can be reasonable when the clusters are roughly uncoupled with the lattice, the electrostatic potential produced by the rest of the lattice is approximately flat and the cluster size is big enough to include a few nearest neighbouring ions. So, the theoretical treatment of this work should be regarded as merely an approximation, and the relative tetragonal elongation obtained by analyzing the EPR spectra is only a tentative result. In order to investigate the local structure and the EPR spectra for the Pt^{3+} center in $BaTiO_3$ to a better extent, the more powerful and reliable density function theory (DFT) approach may be utilized [48–51]. Second, the spectral parameters D_q and N of the similar $\alpha - Al_2O_3 : Pt^{3+}$ [39] adopted here may also introduce some errors into the calculation results. When D_q changes by 10%, the fitted ΔZ and the spin Hamiltonian parameters may vary by about 0.5%, revealing that D_q is somewhat related to the tetragonal distortion and hence to the anisotropy Δg . As N changes by 10%, the errors for the final results are found to be no more than

0.4%, since the covalency affects mainly the average of the g factors. Third, errors may arise from the approximate relation $\bar{A}_2(R) \approx 10.8\bar{A}_4(R)$ for the tetragonal field parameters. The deviation of the relative elongation ΔZ is estimated to be about 3% as the ratio $\bar{A}_2(R)/\bar{A}_4(R)$ varies within the conventional range of 9–12.

4 Conclusion

The microscopic derivation of the improved perturbation formulas for the spin Hamiltonian parameters is presented for a tetragonally elongated $5d^7$ cluster. The theoretical calculations reveal that the Jahn-Teller effect yields 0.05 Å longer $Pt^{3+} - O^{2-}$ bonds along the C_4 axis. Under the uniaxial [001] stress of 0.17 GPa, the impurity center exhibits the moderate decrease of 12% for the tetragonal elongation and the slight increase of 3% for the core polarization constant, resulting in the decline of the anisotropy Δg and the increase of ΔA , respectively.

Acknowledgements This work was financially supported by “the Fundamental Research Funds for the Central Universities”.

References

1. L. Li, Y. Fang, X.M. Chen, J. Am. Ceram. Soc. **95**, 982 (2012)
2. X. Zheng, G. Zheng, Z. Lin, Z. Jiang, Adv. Mater. Res. **485**, 23 (2012)
3. L.G.A. Marques, L.S. Cavalcante, A.Z. Simoes, F.M. Pontes, L.S. Santos-Júnior, M.R.M.C. Santos, I.L.V. Rosa, J.A. Varela, E. Longo, Mater. Chem. Phys. **105**, 293 (2007)
4. M. Ghita, M. Fornari, D.J. Singh, S.V. Halilov, Phys. Rev. B **72**, 54114 (2005)
5. Q. Xu, S. Chen, W. Chen, S. Wu, J. Lee, J. Zhou, H. Sun, Y. Li, J. Alloys Compd. **381**, 221 (2004)
6. R. Jayavel, S. Madeswaran, R.M. Kumar, K. Terabe, K. Kitamura, Mater. Sci. Engin. B **120**, 137 (2005)
7. S. Devi, P. Ganguly, S. Jain, A.K. Jha, Ferroelectrics **381**, 120 (2009)
8. A. Ghemes, Y. Neo, M. Okada, T. Aoki, H. Mimura, Integr. Ferroelectr. **104**, 25 (2008)
9. C. Lu, X.Y. Deng, X.F. Guan, Z.W. Tan, Y.J. Zhang, R.B. Yang, L.R. Han, Adv. Mater. Res. **150**, 599 (2011)
10. G. Yang, Y. Zhou, H. Long, Y. Li, Y. Yang, Thin Solid Films **515**, 7926 (2007)
11. H.T. Langhammer, T. Müller, R. Böttcher, H.P. Abicht, Solid State Sci. **5**, 965 (2003)
12. B. Briat, V.G. Grachev, G.I. Malovichko, O.F. Schirmer, M. Wöhlecke, Defects in Inorganic Photorefractive Materials and Their Applications 2 pp. 9–49 (2002)
13. C. Veber, M. Meyer, O.F. Schirmer, M. Kaczmarek, J. Phys. Condens. Matter **15**, 415 (2003)
14. F. Lin, D. Jiang, X. Ma, W. Shi, J. Magn. Magn. Mater. **320**, 691 (2008)

15. J.R. Sambrano, E. Orhan, M.F.C. Gurgel, A.B. Campos, M.S. Goes, C.O. Paiva-Santos, J.A. Varela, E. Longo, Chem. Phys. Lett. **402**, 491 (2005)
16. Y.C. Huang, W.H. Tuan, Mater. Chem. Phys. **105**, 320 (2007)
17. T.W. Kool, S. Lenjer, O.F. Schirmer, J. Phys. Condens. Matter **19**, 496214 (2007)
18. A. Raizman, A. Schoenberg, J.T. Suss, Phys. Rev. B **20**, 1863 (1979)
19. T. Takeda, A. Watanabe, J. Phys. Soc. Jpn. **21**, 267 (1966)
20. A.S. Chakravarty, *Introduction to the magnetic properties of solids* (Wiley-Interscience Publication, New York, 1980)
21. Y.V. Yablokov, T.A. Ivanova, Coord. Chem. Rev. **190**, 1255 (1999)
22. K.W. Blazey, K.A. Muller, J. Phys. C **16**, 5491 (1983)
23. E. Šimánek, Z. Šroubek, K. Žd'ánský, J. Kaczer, L. Novak, Phys. Status Solidi **14**, 333 (1966)
24. E. Possenriede, P. Jacobs, O.F. Schirmer, J. Phys: Condens. Matter **4**, 4719 (1992)
25. B. Bleaney, A. Abragam, *Electron paramagnetic resonance of transition ions* (Oxford University Press, London, 1970)
26. M.E. Lines, A.M. Glass, *Principles and applications of ferroelectrics and related materials* (Clarendon Press, Oxford, 1977)
27. S.O. Graham, R.L. White, Phys. Rev. B **10**, 4505 (1974)
28. B.R. McGarvey, J. Phys. Chem. **71**, 51 (1967)
29. S.Y. Wu, X.Y. Gao, H.N. Dong, J. Magn. Magn. Mater. **301**, 67 (2006)
30. D.J. Newman, B. Ng, Rep. Prog. Phys. **52**, 699 (1989)
31. D.J. Newman, D.C. Price, W.A. Runciman, Am. Mineral. **63**, 1278 (1978)
32. W.L. Yu, X.M. Zhang, L.X. Yang, B.Q. Zen, Phys. Rev. B **50**, 6756 (1994)
33. H.N. Dong, Y. Wang, L. Sun, D.F. Li, J. Liu, J. Chongqing Univ. Posts Telecommun. **19**, 762 (2010)
34. H.N. Dong, M.R. Dong, J.J. Li, Q.C. Li, H. Xia, J. Chongqing Univ. Posts Telecommun. **24**, 209 (2012)
35. M. Moreno, M.T. Barriuso, J.A. Aramburu, Appl. Magn. Reson. **3**, 283 (1992)
36. R. Weast, CRC Handbook of Chemistry and Physics, CRC Press, Boca Raton, B196, F **187** (1989)
37. E. Clementi, D.L. Raimondi, J. Chem. Phys. **38**, 2686 (1963)
38. E. Clementi, D.L. Raimondi, W.P. Reinhardt, J. Chem. Phys. **47**, 1300 (1967)
39. E. Siegel, K. Müller, Phys. Rev. B **20**, 3587 (1979)
40. C.A. Morrison, *Crystal fields for transition metal ions in laser host materials* (Springer Berlin etc., 1992)
41. E.K. Hodgson, I. Fridovich, Biochem. Biophys. Res. Commun. **54**, 270 (1973)
42. A.K. Koh, D.J. Miller, At. Data Nucl. Data Tables **33**, 235 (1985)
43. A.M. Clogston, V. Jaccarino, Y. Yafet, Phys. Rev. **134**, A650 (1964)
44. A. Abragam, M.H.L. Pryce, Proc. Roy. Soc. (London) A **206**, 164 (1951)
45. S.Y. Wu, W.C. Zheng, P. Ren, Physica B **292**, 337 (2000)
46. K. Sabbe, H. Vrielinck, F. Callens, D. Vandenbroucke, J. Phys. Condens. Matter **12**, 10611 (2000)
47. M. Zdravkova, K. Sabbe, F. Callens, E. Dobbeleir, P. Matthys, Imag. Sci. J. **47**, 63 (1999)
48. M. Moreno, J.A. Aramburu, J.M. Garcia-Lastra, M.T. Barriuso, J. Mol. Structure (Theochem) **759**, 195 (2006)
49. J.A. Aramburu, M.T. Barriuso, P. Garcia Fernández, M. Moreno, Adv. Quant. Chem. **44**, 445 (2003)
50. M.T. Barriuso, J.A. Aramburu, M. Moreno, J. Mol. Structure (theochem) **537**, 117 (2001)
51. J.A. Aramburu, J.I. Paredes, M.T. Barriuso, M. Moreno, Phys. Rev. B **61**, 6525 (2000)